Structures of piperazine, piperidine and morpholine

**Andrew Parkin, Iain D. H.
Oswald and Simon Parsons***

School of Chemistry, University of Edinburgh,
King's Buildings, West Mains Road, Edinburgh
EH9 3JJ, Scotland

Correspondence e-mail: s.parsons@ed.ac.uk

The crystal structures of piperazine, piperidine and morpholine have been determined at 150 K. All three structures are characterized by the formation of NH···N hydrogen-bonded chains. In piperazine these are linked to form sheets, but the chains are shifted so that the molecules interleave. In morpholine there are in addition weak CH···O interactions. Topological analyses show that these three structures are closely related to that of cyclohexane-II, which can be described in terms of a pseudo-cubic close-packed array of molecules in a familiar ABC layered arrangement. While the positions of the molecules within each layer are similar, hydrogen bonding occurs between the ABC layers and in order to accommodate this the molecules are rotated relative to those in cyclohexane-II. Piperidine and morpholine also adopt layered structures, with hydrogen-bonding or CH···O interactions between the layers. In these cases, however, the layering more resembles a hexagonal close-packed arrangement.

1. Introduction

Although cyclohexane is a liquid under ambient conditions, it has been studied extensively by crystallographic methods (Kahn *et al.*, 1973; Wilding *et al.*, 1991, 1993). It exhibits a significant degree of phase diversity, with crystal structures of four polymorphs having been elucidated. Tetrahydropyran and 1,4-dioxane (Buschmann *et al.*, 1986), and 1,3,5-trioxane (Busetti *et al.*, 1969) have also been studied and characterized in the solid state under varying temperature conditions, and these also exhibit several different phases. Little work has as yet been performed to characterize the phase behaviour of heterocyclic cyclohexane analogues possessing groups capable of hydrogen bonding, and structural studies of piperidine, piperazine and morpholine were undertaken with this in mind.

(I)
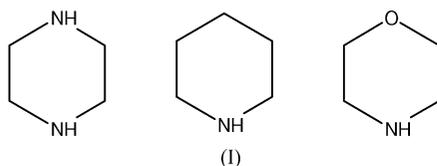
2. Experimental

All materials were obtained from Aldrich and were used as received. The melting points are: piperazine 379 K, piperidine 264 K and morpholine 268 K.

research papers

2.1. Differential scanning calorimetry (DSC)

DSC traces were recorded using a Perkin–Elmer Pyris DSC 1. Samples were contained in open aluminium pans and purged with helium during the temperature scans. The ramping rate was 20 K min^{-1}. The DSC trace for piperidine is shown in Fig. 1. The features in this trace are discussed in §3.2. Traces for morpholine and piperazine revealed no thermal events other than melting or freezing.

2.2. Crystal growth

Colourless block-like crystals of piperazine were grown at room temperature from a saturated solution in ethanol. Piperazine is strongly hygroscopic and prolonged exposure to the air leads to the formation of a hexahydrate (Schwarzenbach, 1968); crystals used for data collection were therefore picked quickly from beneath perfluoropolyether oil. Crystals of both piperidine and morpholine, which are liquids at room temperature, were grown *in situ* on the diffractometer from neat liquids in hand-drawn Pyrex capillaries of approximately 0.3 mm diameter. A single crystal of piperidine suitable for diffraction was obtained by flash-freezing the liquid to form a polycrystalline powder. The sample was held at 250 K and partially melted to leave a small seed crystal by interrupting the cryogenic flow with a spatula. Crystallization was allowed to proceed over a period of 30 min at 250 K. A single crystal of morpholine was obtained in a similar manner, with the polycrystalline powder being held at 269.5 K and the seed crystal being cooled from 269.5 to 259.5 K over a period of 15 min. Samples were cooled to 150 K for data collection.

2.3. Crystallography

X-ray diffraction intensities were collected at 150 K with Mo $K\alpha$ radiation on a Bruker SMART APEX CCD diffractometer equipped with an Oxford Cryosystems low-temperature device (Cosier & Glazer, 1986). Integrations were carried out using *SAINT* (Bruker-AXS, 2002). Absorption corrections were applied using the multiscan procedure *SADABS* (Sheldrick, 1997b, based on the procedure described by Blessing,

1995). All structures were solved by direct methods (*SHELXTL*, Sheldrick, 1997a) and refined by full-matrix least squares against F^2 using all data (*CRYSTALS*; Watkin *et al.*, 2003). H atoms attached to carbon were placed in calculated positions and allowed to ride on their parent atoms with $U_{\mathrm{iso}}(\mathrm{H}) = 1.2U_{\mathrm{iso}}(\mathrm{C})$. H atoms involved in hydrogen bonding were located in difference maps and refined freely. All non-H atoms were modelled with anisotropic displacement parameters. Morpholine crystallized in the non-centrosymmetric space group $P2_12_12_1$, but no attempt was made to refine the Flack parameter (Flack, 1983) because anomalous scattering effects were negligible under the experimental conditions used and thus, Friedel pairs have been merged.

In the case of piperidine, least-squares refinement converged to a relatively high R factor (based on F and all data) of 0.057. Inspection of a plot of F_o^2 against F_c^2 (Fig. 2a) revealed that this was largely owed to a few very strong data. Crystals grown using *in situ* methods are often of very high quality and extinction is often a serious systematic error; although an isotropic extinction correction (Larson, 1970) had been included in the model, these poorly fitting data still had
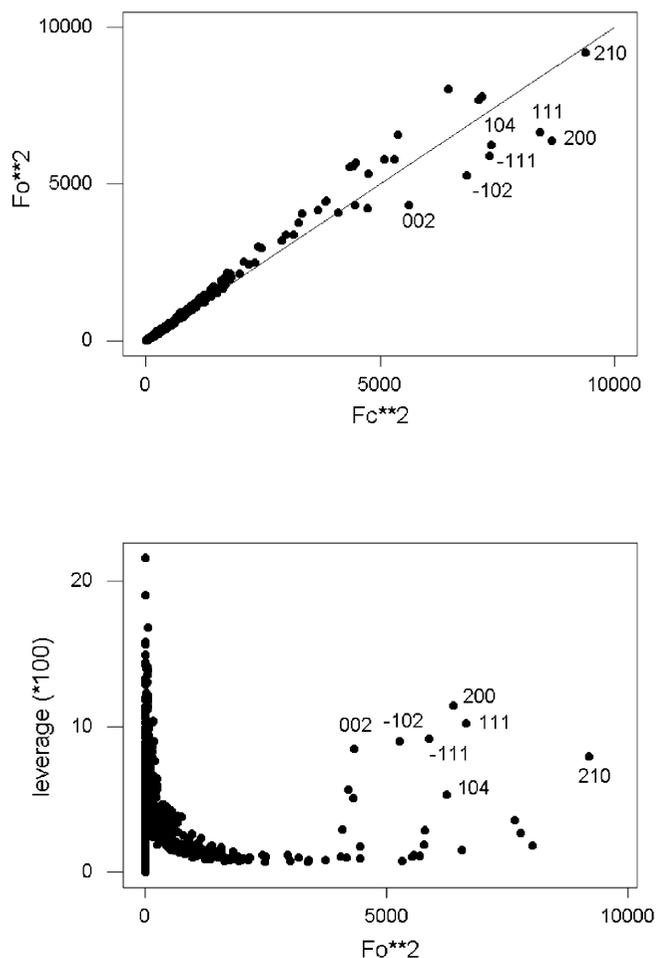
Figure 2
(a) Plot of F_o^2 against F_c^2 for the piperidine data set, showing how a few strong reflections suffering from extinction effects can compromise data fitting for other weaker reflections. (b) Plot of F_o^2 against leverage. The effect of these strong data can be ascribed to their high leverages.

Figure 1
Differential scanning calorimetry trace of piperidine. The lower and upper lines represent the cooling and warming programs, respectively.

Table 1
Experimental details.

	Piperazine	Morpholine	Piperidine
Crystal data			
Chemical formula	$C_4H_{10}N_2$	C_4H_9NO	$C_5H_{11}N$
M_r	86.14	87.12	85.15
Cell setting, space group	Monoclinic, $P2_1/n$	Orthorhombic, $P2_12_12_1$	Monoclinic, $P2_1/c$
a, b, c (Å)	6.0079 (15), 5.1920 (13), 8.407 (2)	5.2311 (5), 8.2292 (7), 11.1370 (10)	8.6989 (7), 5.2642 (4), 12.0097 (10)
β (°)	108.254 (4)	90	96.800 (1)
V (Å^3)	249.05 (11)	479.42 (7)	546.09 (8)
Z	2	4	4
D_x (Mg m^{-3})	1.149	1.207	1.036
Radiation type	Mo $K\alpha$	Mo $K\alpha$	Mo $K\alpha$
No. of reflections for cell parameters	874	3398	2867
θ range (°) for cell	4–27	2–29	2–29
μ (mm^{-1})	0.07	0.09	0.06
Temperature (K)	150	150	150
Crystal form, colour	Plate, colourless	Cylinder, colourless	Cylinder, colourless
Crystal size (mm)	$0.26 \times 0.26 \times 0.03$	$1.00 \times 0.26 \times 0.26$	$1.00 \times 0.30 \times 0.30$
Data collection			
Diffractometer	Bruker SMART	Bruker SMART	Bruker SMART
Data collection method	ω	ω	ω
Absorption correction	Multi-scan (based on symmetry-related measurements)	Multi-scan (based on symmetry-related measurements)	Multi-scan (based on symmetry-related measurements)
T_{min}	0.813	0.824	0.924
T_{max}	1.000	1.000	1.000
No. of measured, independent and observed reflections	1431, 511, 413	4211, 703, 655	4925, 1319, 1145
Criterion for observed reflections	$I > 2.00u(I)$	$I > 2.00u(I)$	$I > 2.00u(I)$
R_{int}	0.011	0.030	0.032
θ_{max} (°)	26.4	28.7	28.7
Range of h, k, l	$-6 \Rightarrow h \Rightarrow 7$	$-6 \Rightarrow h \Rightarrow 6$	$-11 \Rightarrow h \Rightarrow 11$
	$-3 \Rightarrow k \Rightarrow 6$	$-10 \Rightarrow k \Rightarrow 10$	$-6 \Rightarrow k \Rightarrow 7$
	$-10 \Rightarrow l \Rightarrow 10$	$-14 \Rightarrow l \Rightarrow 14$	$-15 \Rightarrow l \Rightarrow 15$
Refinement			
Refinement on	F^2	F^2	F^2
$R[F^2 > 2\sigma(F^2)]$, $wR(F^2)$, S	0.036, 0.087, 0.94	0.044, 0.106, 1.11	0.042, 0.120, 1.02
No. of reflections	511	699	1319
No. of parameters	32	60	59
H-atom treatment	Not refined/refined independently	Not refined/refined independently	Mixture of independent and constrained refinement
Weighting scheme	$w = 1/[\sigma^2(F_o^2) + (0.05P)^2]$, where $P = \frac{1}{3}\max(F_o^2, 0) + \frac{2}{3}F_c^2$	$w = 1/[\sigma^2(F_o^2) + (0.03P)^2 + 0.15P]$, where $P = \frac{1}{3}\max(F_o^2, 0) + \frac{2}{3}F_c^2$	$w = 1/[\sigma^2(F_o^2) + (0.06P)^2 + 0.08P]$, where $P = \frac{1}{3}\max(F_o^2, 0) + \frac{2}{3}F_c^2$
$(\Delta/\sigma)_{max}$	<0.0001	0.001	<0.0001
$\Delta\rho_{max}$, $\Delta\rho_{min}$ (e Å^{-3})	0.16, −0.14	0.19, −0.24	0.23, −0.13
Extinction method	Larson (1970), eq 22	Larson (1970), eq 22	None
Extinction coefficient	15.207	166.7 (309)	–

Computer programs used: *SMART* (Bruker-AXS, 2002), *SAINT* (Bruker-AXS, 2002), *SHELXTL* (Sheldrick, 1997a), *CRYSTALS* (Watkin *et al.* 2003), *CAMERON* (Watkin *et al.* 1993).

F_o^2 significantly less than F_c^2 (Fig. 2a). A leverage analysis (Prince, 1994; carried out using a locally written program) suggested that these data also had very high leverages and their systematic error compromised the fitting of other weaker reflections (Fig. 2b). Omission of these data (14 reflections in all) led R to drop to a more acceptable 0.047. The extinction parameter was subsequently removed from the model after assuming a physically unreasonable, negative, value.

A full listing of crystal, data collection and refinement parameters is given in Table 1; a set of hydrogen-bonding parameters are given in Table 2; primary bond distances and angles are available in the supplementary data.[1] Crystal packing was investigated using the program *Mercury* (Bruno *et al.*, 2002), and figures were produced using *SHELXTL* or *CAMERON* (Watkin *et al.*, 1993). Other analyses utilized the p.c. version of the program *PLATON* (Spek, 2002; Farrugia, 1999). Puckering parameters were calculated using the program *PUCKER* (Gould *et al.*, 1995).

A new facility in *CRYSTALS* interfaces with *MOGUL*, a library of information about molecular geometry taken from the Cambridge Database (Cambridge Crystallographic Data Centre, 2003; Cooper, 2001). This enables primary bond distances and angles to be quickly compared with those in

[1] Supplementary data for this paper are available from the IUCr electronic archives (Reference: AV5005). Services for accessing these data are described at the back of the journal.

Table 2
Hydrogen bonding and other intermolecular contact parameters in piperazine, piperidine and morpholine (Å, °).

Standard uncertainties were calculated using the full variance–covariance matrix, but are only quoted if all atoms involved were refined freely. The sums of the van der Waals radii of N and H, and O and H are 2.75 and 2.72 Å, respectively. In each case the primary graph-set descriptor is $C(2)$.

Piperazine		Piperidine		Morpholine	
H1$\cdots$N1[i]	2.319 (16)	H1$\cdots$N1[ii]	2.346 (13)	H4$\cdots$N4[iii]	2.35 (3)
N1$\cdots$N1[i]	3.186 (1)	N1$\cdots$N1[ii]	3.185 (1)	N4$\cdots$N4[iii]	3.232 (2)
∠N1H1$\cdots$N1[i]	170.3 (12)	∠N1H1$\cdots$N1[ii]	169.8 (10)	∠N4H4$\cdots$N4[iii]	169 (2)
		O1$\cdots$H51[iv]	2.63		
		O1$\cdots$C5[iv]	3.510 (3)		
		∠O1$\cdots$H51C5[iv]	150		

Symmetry operations: (i) $\frac{3}{2} - x, -\frac{1}{2} + y, \frac{1}{2} - z$; (ii) $1 - x, -\frac{1}{2} + y, \frac{1}{2} - z$; (iii) $\frac{1}{2} + x, -\frac{1}{2} - y, -z$; (iv) $-x, \frac{1}{2} + y, \frac{1}{2} - z$.

Table 3
Topological properties of the crystal structures of cyclohexane-II (C_6H_{12}), piperazine ($C_4H_{10}N_2$), piperidine ($C_5H_{11}N$) and morpholine (C_4H_9NO).

CS represents the coordination sequence, *i.e.* the number of molecules in the first, second and third coordination shells. K_{cov} and K_{pack} are the covering and packing coefficients, respectively. The superscript [a] indicates that all Voronoi–Dirichlet polyhedron faces were taken into account in the calculation, [b] indicates that two faces which were much smaller than the others were omitted. For example, in the case of cyclohexane-II, two contacts made lattice VDP faces with areas of 0.24% of the full solid angle ($4\pi sr$), while the next smallest faces had areas of 3.97% of the full solid angle. There were no small faces in the lattice VDP of piperazine. Notice that quite similar results are obtained for both the smoothed and lattice VDP analyses; this is to be expected for small molecules such as these and deviations become more significant as molecules become less isometric. Coordination sequences for perfect body-centred cubic, cubic close-packed and hexagonal close-packed structures are 14–50–110, 12–42–92 and 12–44–96, respectively (Blatov, 2001; Peresypkina & Blatov, 2000b). The continuous symmetry measures of the distributions of centroids in piperazine, piperidine and morpholine are 2.2 (relative to c.c.p.), 2.0 (h.c.p.) and 1.4 (h.c.p.).

	Smoothed VDP analysis			Lattice VDP analysis			
Compound	CS[a]	CS[b]	K_{cov}[a]	CS[a]	CS[b]	K_{cov}[a]	K_{pack}
C_6H_{12}-II	14–50–110	12–42–92	1.93	14–50–110	12–42–92	1.93	0.71
$C_4H_{10}N_2$	14–54–124	12–42–92	2.15	12–42–92	–	2.12	0.71
$C_5H_{11}N$	14–54–126	12–44–96	2.13	14–52–116	12–44–96	2.05	0.66
C_4H_9NO	14–52–116	12–44–96	1.95	14–52–116	12–44–96	1.95	0.70

similar moieties; a combined figure of merit is generated for the bond distances and angles about each atom based on values of $Z = |X_{obs} - X_{median}|/\sigma$ for each parameter involving that atom (X_{obs} is the observed value for a distance or angle, X_{median} is the median value for that type of distance or angle in the CSD and σ is the standard deviation of the MOGUL distribution). Values of Z greater than 3 may indicate unusual geometry. This facility is extremely useful for checking whether geometrical parameters have assumed unusual values (Cooper, 2001).

2.4. Topological calculations

Topological analyses were carried out using the TOPOS3.1 program suite (Blatov *et al.*, 1999). Adjacent matrices were calculated using the program AUTOCN using the method of spherical sectors; the minimum solid angle of a Voronoi–Dirichlet polyhedron (VDP) face corresponding to an intermolecular contact was set to zero. Analysis of both smoothed

and lattice VDPs were carried out with the program *ADS*, with the geometrical centres of the molecules (as opposed to their centres of gravity) as reference points. Coordination sequences were calculated out to three coordination spheres. In each case two sets of calculations were carried out: one in which all VDP faces were taken into account, and another in which very small VDP faces were omitted. Results for piperazine, morpholine, piperidine and cyclohexane-II are presented in Table 3 and illustrated in Fig. 3. Full details of these procedures can be found in the TOPOS3.1 manual, and in papers by Blatov and co-workers (for example, Blatov, 2001; Peresypkina & Blatov, 1999, 2000a,b).

Calculations of continuous symmetry measures were carried out using a locally written program using the method described by Pinsky & Avnir (1998). Molecular volumes (V_{mol}) for packing coefficient calculations (see Table 3) were obtained using $CERIUS^2$ (Molecular Simulations Inc., 1999). The packing coefficient is defined as ZV_{mol}/V_{cell}, where V_{cell} is the volume of the unit cell and Z the number of molecules per cell (Kitaigorodski, 1973).

3. Results

3.1. Piperazine

Piperazine crystallizes from ethanol under ambient conditions in the space group $P2_1/n$. The molecule resides on a crystallographic inversion centre and has the ideal chair conformation with N—H bonds in the equatorial positions (Fig. 4a). The maximum MOGUL combined figure-of-merit was 1.36, indicating that the bond distances and angles in piperazine are normal. N—H$\cdots$N hydrogen-bonding interactions, measuring 2.319 (16) Å, are formed between molecules (Table 2, Fig. 4b); the primary graph-set descriptor is a $C(2)$ chain which is built along the 2_1 axes (Bernstein *et al.*, 1995). These chains are related to other $C(2)$ chains by the crystallographic inversion centres located at the centres of the molecules. The overall effect is to build up layers of molecules which lie parallel to the ($\bar{1}01$) planes (Fig. 4c). The distance between successive planes of molecular centroids is 5.53 Å.

3.2. Piperidine

Piperidine is structurally related to piperazine by the substitution of one NH group by CH_2. It crystallizes in the space group $P2_1/c$ with one molecule per asymmetric unit occupying a general position. Like piperazine, it has a chair conformation (95% of the puckering can be described with an ideal cyclohexane chair) with the H atom in an equatorial position (Fig. 5a). Primary bond distances and angles are

unremarkable (maximum MOGUL combined figure-of-merit = 1), and a listing is available in the supplementary data. As in piperazine the most significant intermolecular interaction is an N—H···N hydrogen bond, which measures 2.346 (13) Å (Table 2, Fig. 5b). This similarity with piperazine also extends to the primary graph set, which is comprised by $C(2)$ chains disposed about the crystallographic 2_1 axes. The substitution of NH by CH_2 in the 4-position disrupts the layer structure observed in piperazine. Projection of the structure onto the ac plane reveals a close-packed-like arrangement of chains; perpendicular to this direction the piperidine molecules in neighbouring chains are interleaved (Fig. 5c).

The melting point of piperidine is 250 K, although under cooling conditions of the DSC experiment the sample did not freeze until 244 K (Fig. 1). A phase transformation occurred at 239 K. This second phase is stable to cooling to 120 K and is presumably that described in this paper. The first phase was not recovered by warming the second phase above 238 K.

3.3. Morpholine

Morpholine is structurally related to piperazine by the substitution of one NH group by oxygen. It crystallizes at 267 K in the space group $P2_12_12_1$ with one molecule per asymmetric unit occupying a general position. The maximum *MOGUL* combined figure-of-merit for primary bond distances and angles was 1.0. Like piperazine and piperidine, it has a chair conformation (98% of the puckering can be described with an ideal cyclohexane chair) with the H atom in an equatorial position (Fig. 6a); primary bond distances and angles are available in the supplementary data. The C2—

Figure 3
Lattice Voronoi–Dirichlet polyhedra in: (a) body-centred cubic packing; (b) cubic close-packing; (c) hexagonal close-packing; (d) cyclohexane-II – all faces shown, note the presence of two small faces; (e) cyclohexane-II with small faces removed, cf. (b); (f) piperazine; (g) piperidine; (h) morpholine. *Combinatorial types* (Peresypkina & Blatov, 2000a) can be written $f/v - n$, where f is the number of faces and v the number of vertices; n is just an ordinal number to distinguish different VDPs where f and v are equal. These are: (a) 14/24–1, (b) 12/14–1, (c) 12/14–2, (d) 14/24–1, (e) 12/20–2, (f) 12/18–1, (g) 12/20–1 and (h) 12/20–1. Differences arise in the number of vertices present in related structures, e.g. compare the top-left vertices of (b) and (e).

Figure 4
The crystal structure of piperazine. (a) Molecular displacement ellipsoids are drawn at the 30% probability level; H atoms are drawn as circles of arbitrary radius. (b) Packing viewed along **b**, showing the formation of hydrogen-bonded layers. (c) One layer projected onto ($\bar{1}$01); the **b** direction runs approximately vertically.

NH—NH— chains which characterized the structures of piperazine and piperidine are also observed in morpholine. The NH···N distance is 2.35 (3) Å (Table 2). Packing of the chains is reminiscent of those in piperidine, except that they are oriented in such a way that weak CH···O interactions (2.63 Å) are formed between the molecules in neighbouring chains (Fig. 6b).

4. Discussion

4.1. General structural features and phase behaviour

Although amines are fairly weak hydrogen-bond donors, they are strong acceptors, and piperazine, piperidine and morpholine all exhibit chain-like structures developed through NH···N hydrogen bonds. NH···O hydrogen bonding is in principle possible in morpholine, although the stronger acceptor character of amine *versus* ether is presumably the reason that this is not observed. The N···N distances in the three structures vary only slightly (range: 3.18–3.23 Å) and the distances compare closely with a mean [3.22 (14) Å] for such interactions in the Cambridge Database (Allen, 2002; Version 5.24, November 2002). Morpholine exhibits weak CH···O interactions in which the H···O distance (2.63 Å) is slightly less than the sum of the van der Waals radii of H and O (2.72 Å). Although this interaction must be very weak, in the crystal structure the molecules of morpholine do seem to be oriented in order to engage in it, and interactions of similar dimensions are observed in the crystal structures of 1,4-

Figure 5
The crystal structure of piperidine. (a) Molecular displacement ellipsoids are drawn at the 30% probability level; H atoms are drawn as circles of arbitrary radius. (b) Packing viewed along **b**, showing the formation of hydrogen-bonded chains. (c) One layer projected along **c** showing the interleaving of chains.
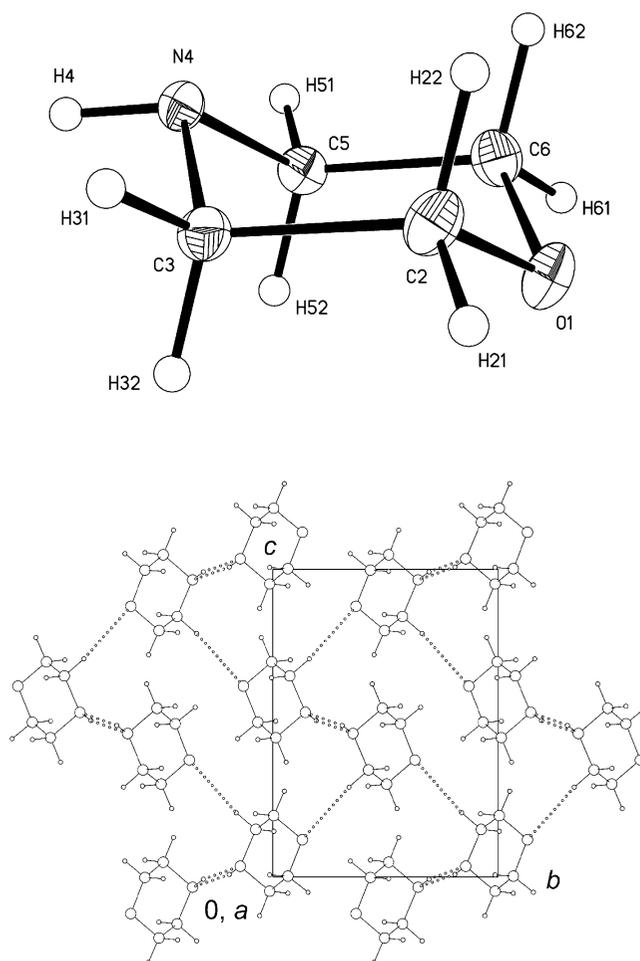
Figure 6
The crystal structure of morpholine. (a) Molecular structure. Displacement ellipsoids are drawn at the 30% probability level; H atoms are drawn as circles of arbitrary radius. (b) Packing viewed along **a**, showing the formation of hydrogen-bonded chains linked by long CH···O interactions.

dioxane (CSD refcodes CUKCIU and CUKCIU01; Buschmann *et al.*, 1986).

Differential scanning calorimetry measurements show that piperidine appears to form one phase on cooling from the liquid, which then transforms to the phase described here at 239 K. However, the higher temperature phase cannot be recovered by warming the low-temperature phase to 238 K, although a shoulder on the melting transition suggests that some phase alteration may occur immediately prior to melting.

A further very weak transition occurs at 219 K. The formation of the first phase appears to depend on experimental conditions and is not always observed. On our first attempt to crystallize piperidine we measured metrically monoclinic primitive unit-cell dimensions of $a = 7.033$ (3), $b = 5.224$ (3), $c = 7.852$ (4) Å and $\beta = 108.03$ (3)°. The crystal was of low quality, however, and data collection on this sample was not pursued. Sadly, we have been unable to repeat this result. Similar behaviour is observed in acetone (Allan *et al.*, 1999). We are currently investigating the phase behaviour of this compound more closely.

(a)

A

B

C

(b)
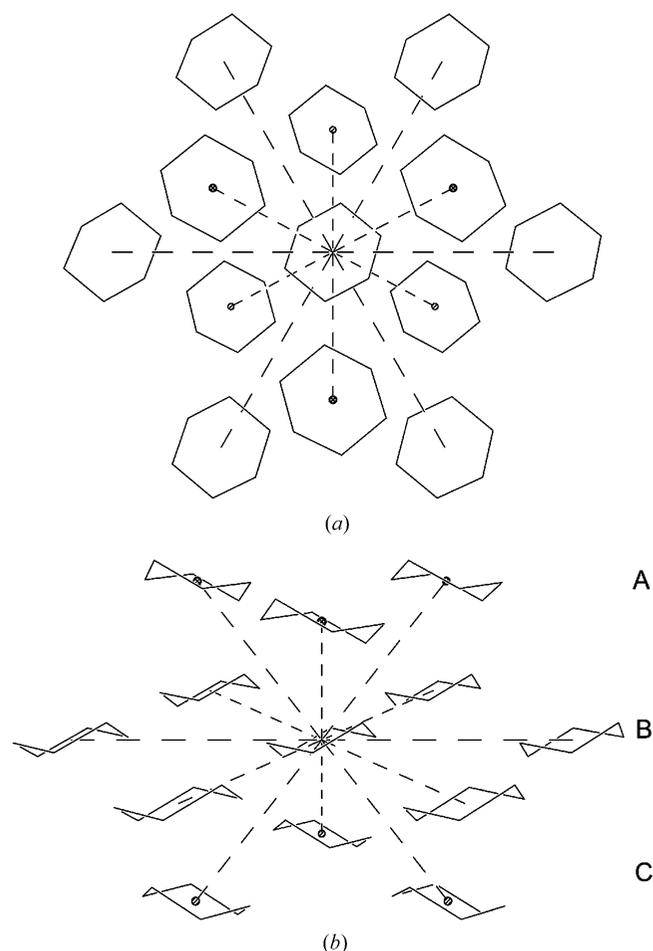
Figure 7
Molecular coordination in cyclohexane-II (CSD refcode: CYCHEX). The distribution of the molecular centroids resembles that in a cubic close-packed structure, with layers following an ...*ABCABC*... pattern. Layers viewed from the top (*a*) and side (*b*). Centroids in layers A and C are marked with a circle containing a cross (top layer) or a diagonal line (bottom layer), respectively. H atoms are omitted for clarity.

4.2. Structural relationship with cyclohexane

The three compounds studied here are related to cyclohexane by the substitution of one or more of the CH_2 groups for NH and/or O, and it might be anticipated that some relationship should exist between the crystal structures of all four compounds. Cyclohexane has a rich phase diversity and it has been studied under varying degrees of temperature and pressure. Phase I, which occurs between the melting point (279.82 K) and 186.1 K, is a plastic phase crystallizing in the space group $Fm\bar{3}m$, in which the molecules undergo rapid molecular reorientations about the lattice points. On cooling below 186.1 K an order–disorder transition occurs to give phase II (space group $C2/c$; Kahn *et al.*, 1973). The application of pressure to cyclohexane-d_{12} initially yields phase I at 5 kbar and room temperature, but this transforms to phases III ($Pmnn$) and IV ($P2_1/n$) at 280 and 250 K, respectively (Wilding *et al.*, 1991, 1993). Phase IV has also been observed at ambient pressure by rapidly cooling cyclohexane-h_{12} to 77 K.

The coordination environment of a molecule in a crystal structure can be visualized using a Voronoi–Dirichlet polyhedron or VDP (Peresypkina & Blatov, 2000a,b). Voronoi–Dirichlet analysis is a method for partitioning space amongst points which occupy that space. A point is separated from a neighbouring point by a plane which bisects the vector between them. This construction is repeated for every pair of points to yield a subdivision of the space into cells which each contain one point. VDP analysis carried out using individual atoms to define the points leads to a *molecular* VDP. In general, the molecular VDP is non-convex (see, for example, Fig. 2 in Peresypkina & Blatov, 2000a). If the VDP is constructed using only the molecular centroids, the result is a convex *lattice* VDP. This characterizes the topology of crystal packing. In cases of crystal structures of non-isometric mole-

A

B

C
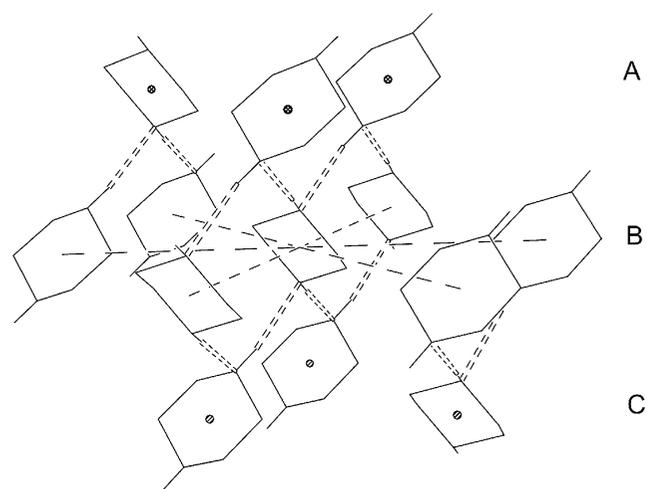
Figure 8
Molecular coordination in piperazine. This figure should be compared with Fig. 7(*b*). Molecular coordination paths are indicated with a dashed line; links to the top and bottom layers have been omitted for clarity, although the centroids in these layers are indicated with filled circles. Hydrogen bonds are shown with a double dashed line. Layers in this structure may be chosen in several different ways; those shown in Fig. 4(*c*) run vertically in this figure. H atoms attached to C are omitted for clarity.

cules VDP faces corresponding to the intermolecular contacts may be lost during this construction. If these interactions are taken into account, then the result is a *smoothed* VDP. The number of faces of the smoothed VDP is the molecular coordination number. Smoothed VDPs do not, however, always yield a complete partitioning of space.

Although cyclohexane-I has a low packing coefficient (0.62), and cannot be described as 'close-packed', the coordination number of the average positions is 12, with a distribution which follows the familiar *ABC* layering characteristic of a cubic close-packed (c.c.p.) hard-sphere structure. The results of the topological VDP analysis presented in Table 3 show that the coordination sequence (whether calculated using smoothed or lattice VDPs) in cyclohexane-II is 14–50–110; that is, there are 14 molecules in the first coordination sphere, 50 in the second and 110 in the third. This makes the structure topologically equivalent to a body-centred cubic (b.c.c.) hard-spheres structure. However, two centroid-to-centroid intermolecular distances are very long compared with the other 12 (7.95 compared with 5.21–6.47 Å) and omitting these from the calculation yields a coordination sequence of 12–42–92, which is characteristic of a cubic close-packed (c.c.p.) structure. The lattice VDP of cyclohexane-II is compared with those of perfect b.c.c. and c.c.p. in Fig. 3, and it clearly resembles the latter more closely. This interpretation of the topology is supported by the covering coefficient (K_{cov}), defined by Blatov as V_s/V_{VDP}, where V_{VDP} is the volume of the VDP and V_s is the volume of the sphere circumscribed around it. K_{cov} adopts a value of 1.46 for a perfect b.c.c. structure and 2.09 for a close-packed structure; with a value of 1.93 cyclohexane-II more resembles the latter.

The molecular centroids in cyclohexane-II thus retain a coordination number of 12 with the *ABC* layered arrangement present in the plastic phase (I) (Fig. 7). This is also the case for cyclohexane-III and cyclohexane-IV. The deviation of the distribution of the molecular centroids from perfect c.c.p. can be quantified using the continuous symmetry measure parameter described by Pinsky & Avnir (1998). In general, this measure has a physical bound of 0 to 100, and we obtain values of 2.0, 0.9 and 1.1 for cyclohexane-II, -III and -IV, respectively, where a value of 0.0 corresponds to perfect c.c.p. Cyclohexane-III and -IV are both high-pressure polymorphs and the distribution of their centroids more closely resembles perfect c.c.p. than in cyclohexane-II; this often seems to be the case in crystal structures determined at high pressure.
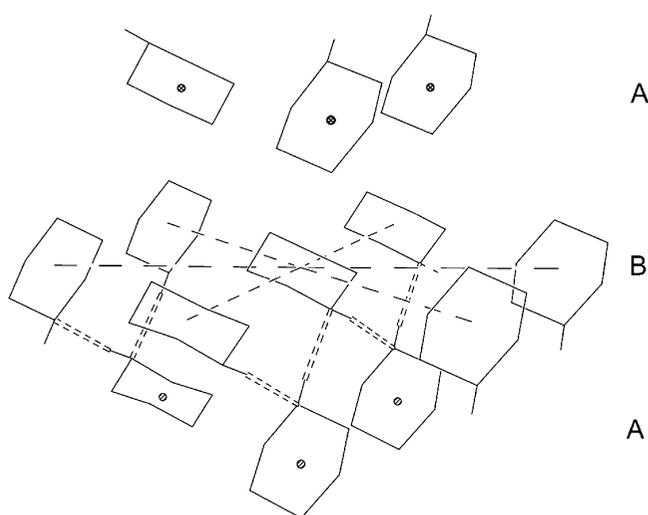
The crystal structures of piperazine, piperidine and morpholine also contain molecules which, although formally 14-coordinate, exhibit two centroid-to-centroid distances much longer than the other 12, and in all three structures the molecular coordination number is best considered to be 12. Lattice VDP plots are shown in Figs. 3(*f*)–(*h*). The molecular centroids in piperazine also adopt a *CCP* distribution (coordination sequence 12–42–92), with a continuous symmetry measure of 2.2 relative to a c.c.p. structure. While the positions of the molecules within each layer are similar to those in cyclohexane-II, hydrogen bonding occurs between the *ABC* layers and in order to accommodate this the molecules are rotated relative to those in cyclohexane-II (Fig. 8). Since there are four threefold rotational axes of symmetry in a c.c.p. structure, these layers can be chosen in four different ways. The choice here was made to facilitate comparison with morpholine and piperidine, and in the latter hydrogen bonds can be considered to be formed between alternate layers (Fig. 9). Piperidine is therefore a kind of hybrid between the cyclohexane and piperazine structures, as would be expected on the basis of the molecular structures.

Figure 9
Molecular coordination in piperidine. This figure should be compared with Figs. 7(*b*) and 8. Molecular coordination paths are indicated with a dashed line; links to the top and bottom layers have been omitted for clarity, although the molecular centroids in these layers are indicated with filled circles. Hydrogen bonds are shown with a double dashed line. H atoms attached to C are omitted for clarity.

Figure 10
Molecular coordination in morpholine. This figure should be compared with Figs. 7(*b*), 8 and 9. Molecular coordination paths are indicated with a dashed line; links to the top and bottom layers have been omitted for clarity, although the molecular centroids in these layers are indicated with filled circles. Hydrogen bonds are shown with a double dashed line; long CH⋯O interactions are shown with heavy dashed lines. H atoms not attached to nitrogen have been omitted.

The piperazine and cyclohexane structures both consist of centrosymmetric molecules with their centroids on inversion centres. The piperidine molecule is non-centrosymmetric and in its (centrosymmetric) crystal structure the inversion centres lie between molecules. This is incompatible with a c.c.p. distribution of centroids and piperidine therefore adopts a hexagonally close-packed (h.c.p.) arrangement (coordination sequence 12–44–96), with a continuous symmetry measure of 2.0 relative to perfect h.c.p. The crystal structure of morpholine is non-centrosymmetric (space group $P2_12_12_1$). This is a common space group for molecules which lack inversion symmetry and it is usually the case that in this space group molecules tend to avoid the screw axes (Motherwell, 1997). Here the molecules lie very close to the unit-cell origin and if only the molecular centroids are considered the space group is $Pnma$, with the centroids lying on mirror planes either side of the inversion centres. The packing in morpholine yields a coordination sequence of 12–44–96 and this structure can therefore also be considered to be based on h.c.p.; this is illustrated in Fig. 10. The continuous symmetry measure is 1.4 relative to perfect h.c.p. Both NH···N and CH···O hydrogen bonds are formed between the layers.

Although recent work by Peresypkina & Blatov (2000a,b) and other workers reveals that the molecular coordination number 14 is most common in molecular crystal structures, 12 is far from rare. Indeed, Kitaigorodski (1973) noted that 12 was most common, although this may have been dependent on his method of calculation. There is a clear relationship between the crystal structures of cyclohexane-II, piperazine, piperidine and morpholine, all forming layered structures with either a c.c.p. or h.c.p. distribution of molecular centroids depending on whether these coincide with a molecular inversion centre. All four molecules have packing coefficients in Kitaigorodski's typical range (0.65–0.77: cyclohexane-II and piperazine, 0.71; piperidine, 0.66, and morpholine, 0.70), although piperidine is notably rather low and this perhaps explains why at least two different phases are observed between 77 K and its melting point.

References

Allan, D. R., Clark, S. J., Ibberson, R. M., Parsons, S., Pulham, C. R. & Sawyer, L. (1999). *Chem. Commun.* pp. 751–752.
Allen, F. H. (2002). *Acta Cryst.* B**58**, 380–388.
Bernstein, J., Davis, R. E., Shimoni, L. & Chang, N.-L. (1995). *Angew. Chem. Int. Ed. Engl.* **34**, 1555–1573.
Blatov, V. A. (2001). *Z. Kristallogr.* **216**, 165–171.
Blatov, V. A., Shevchenko, A. P. & Serezhkin, V. N. (1999). *J. Appl. Cryst.* **32**, 377.
Blessing, R. H. (1995). *Acta Cryst.* A**51**, 33–38.
Bruker-AXS (2002). *SAINT*, Version 6. Bruker-AXS, Madison, Wisconsin, USA.
Bruno, I. J., Cole, J. C., Edgington, P. R., Kessler, M., Macrae, C. F., McCabe, P., Pearson, J. & Taylor, R. (2002). *Acta Cryst.* B**58**, 389–397.
Buschmann, J., Müller, E. & Luger, P. (1986). *Acta Cryst.* C**42**, 873–876.
Busetti, V., Del Pra, A. & Mammi, M. (1969). *Acta Cryst.* B**25**, 1191–1194.
Cambridge Crystallographic Data Centre (2003). *MOGUL.* Molecular geometry library suitable for very rapid searching.
Cooper, R. I. (2001). PhD Thesis. University of Oxford, England.
Cosier, J. & Glazer, A. M. (1986). *J. Appl. Cryst.* **19**, 105–107.
Farrugia, L. J. (1999). *J. Appl. Cryst.* **32**, 837–838.
Flack, H. D. (1983). *Acta Cryst.* A**39**, 876–881.
Gould, R. O., Taylor, P. & Thorpe, M. (1995). *PUCKER.* The University of Edinburgh, Scotland.
Kahn, R., Fourme, R., André, D. & Renaud, M. (1973). *Acta Cryst.* B**29**, 131–138.
Kitaigorodski, A. I. (1973). *Molecular Crystals and Molecules.* New York: Academic Press.
Larson, A. C. (1970). *Crystallogr. Comput. Proc. Int. Summer Sch.* pp. 291–294.
Molecular Simulations Inc. (1999). *Cerius*^{2}. Molecular Simulations Inc., San Diego, CA, USA.
Motherwell, W. D. S. (1997). *Acta Cryst.* B**53**, 726–736.
Peresypkina, E. V. & Blatov, V. A. (1999). *J. Mol. Struct. (Theochem.)* **489**, 225–236.
Peresypkina, E. V. & Blatov, V. A. (2000a). *Acta Cryst.* B**56**, 501–511.
Peresypkina, E. V. & Blatov, V. A. (2000b). *Acta Cryst.* B**56**, 1035–1045.
Pinsky, M. & Avnir, D. (1998). *Inorg. Chem.* **37**, 5575–5582.
Prince, E. (1994). *Mathematical Techniques in Crystallography and Materials Science*, 2nd Ed. Berlin: Springer-Verlag.
Schwarzenbach, D. (1968). *J. Chem. Phys.* **48**, 4134–4140.
Sheldrick, G. M. (1997a). *SHELXTL.* Bruker-AXS, Madison, Wisconsin, USA.
Sheldrick, G. M. (1997b). *SADABS.* Bruker-AXS, Madison, Wisconsin, USA.
Spek, A. L. (2002). *PLATON.* Utrecht University, The Netherlands.
Watkin, D. J., Pearce, L. & Prout, C. K. (1993). *CAMERON.* Chemical Crystallography Laboratory, University of Oxford, England.
Watkin, D. J., Prout, C. K., Carruthers, J. R., Betteridge, P. W. & Cooper, R. I. (2003). *CRYSTALS*, Issue 12. Chemical Crystallography Laboratory, Oxford, UK.
Wilding, N. B., Crain, J., Hatton, P. D. & Bushnell-Wye, G. (1993). *Acta Cryst.* B**49**, 320–328.
Wilding, N. B., Hatton, P. D. & Pawley, G. S. (1991). *Acta Cryst.* B**47**, 797–806.